Colloid Polym Sci 280:661–673 (2002)
© Springer-Verlag 2002

ORIGINAL CONTRIBUTION

H. G. Kilian

Carbon blacks as dissipative colloid systems with universal properties

Received: 17 April 2001
Accepted: 1 August 2001

H.G. Kilian
Abteilung Experimentelle Physik
Universität Ulm, 89069 Ulm, Germany
e-mail:
hanns-georg.kilian@physik.uni-ulm.de

Abstract As a new approach the stationary size distribution of particles and aggregates of particles of carbon blacks is described with an extended version of the model of reversible aggregation. Computer simulations of aggregation in dissipative systems lead to ensembles the reduced size distributions of which are at not too short times identical with the universal stationary distribution of the aggregation model. A crucial general point seems to be that structural fluctuations activated by continuously running chemical reactions including viscous dissipation exhibits the same statistics as it is typical for thermally activated aggregation. This leads to the suggestion that the production of carbon blacks at very high temperatures or the reorganization during the so-called CAB-procedure should show a statistically analogous fluctuation-dissipation behaviour as thermally activated aggregation. The ensemble entropy is, in any case, rapidly maximized. In the reactor, for example, a sequence of generations with quasi-stationary ensemble structures is finally built up. Dissipation-fluctuation, including highly cooperative phenomena, guarantees a unique and optimized stationary, thermodynamically "essentially entropy controlled" colloid-structure. Universality is impressively verified by the finding that the particle and aggregate size distributions of different carbon blacks belong to the same "class" so that their reduced representations fall altogether on a master curve. Consequences of our interpretation are discussed.

Keywords Reversible aggregation · Dissipative systems · Carbon-blacks · Particles · Aggregates · Size-distributions

Introduction

Dry carbon blacks exhibit stationary aggregate ensembles as shown in Fig. 1 [1, 2]. Each aggregate is comprised of a decent number of "primary particles" (calling them here "particles"). In Fig. 2 the mass fractions of aggregates of different carbon blacks [3] are plotted against the diameter. The similarity of the distributions is evidenced at a first view. The particles also exhibit a size distribution [4] (Fig. 3) with a shape which compares with the one of aggregates. The distributions tend to be positively skewed, i.e. they contain higher populations of particles or aggregates in the smaller diameter regime than at the larger end of the distribution. It is remarkable that the hierarchically organized colloid structure of carbon blacks is generated within very short periods of time (μseconds!) [5].

Theories of the formation of carbon black particles or aggregates of carbon blacks [5] have not been developed to an accepted general version [6]. This is, of course, closely related to the complexity of the processes. Informative is the observation that in the reactor at high temperatures the concentration of the poly-acetylene goes through a maximum early in the reaction zone and reaches a

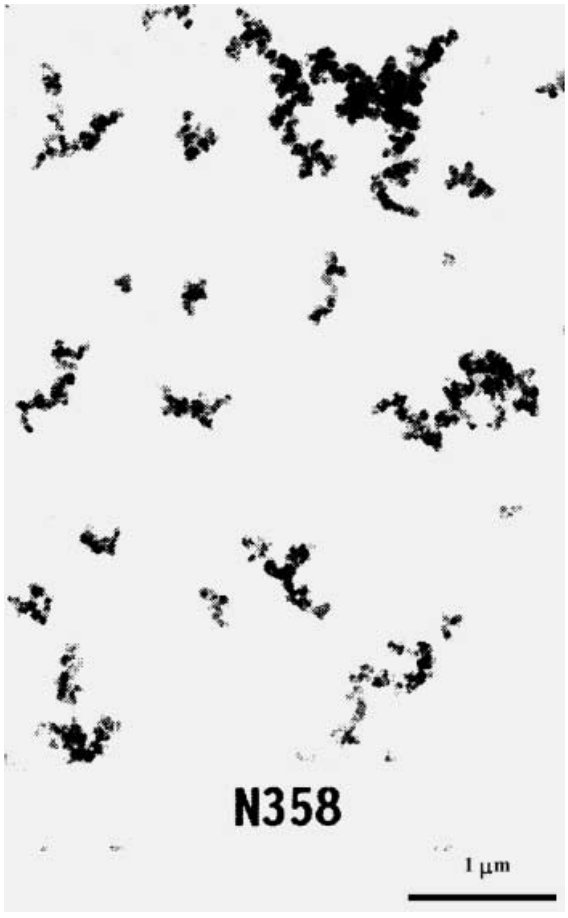

Fig. 1 Transmission electron microscopic picture of carbon black N358 according to [3]

constant final value in the burnt gas [7]. In the region where the poly-acetylene concentration decreases, the size of the particles increases by aggregation of smaller particles and by addition of higher poly-acetylenes and poly-acetylene radicals. The number density of carbon particles goes down finally reaching a stage where the mean particle diameter and the particle number attain a constant value [5]. The reaction arrives at a stationary limit producing a defined pattern of particles and aggregates (their absolute properties depend, of course, on the reaction conditions).

Another relevant observation should be discussed here. Submitted to the so-called "CAB-procedure" (peculiar dispersion procedure in cellulose acetate butyrate (CAB) at about 450 K [8]) the original patterns suffer an extensive breakdown of the dry carbon black aggregates. The mean size of aggregates and the width of the size distribution are substantially reduced (Fig. 4).

The conception

Let us first debate aggregate ensembles (Fig. 1). In terms of an increment model the number of particles y_a should characterize the size of an aggregate. The mean energy of particle-particle contacts is supposed to be the same. At the moment, we consider thermally activated processes. If the aggregation standard energy is smaller than the mean thermal energy $1/\beta = k_B T$ (stored via continuously running fluctuation-dissipation processes) reversible aggregation can be activated, i.e. aggregates can be formed or annihilated. Each aggregate has thus a finite lifetime.

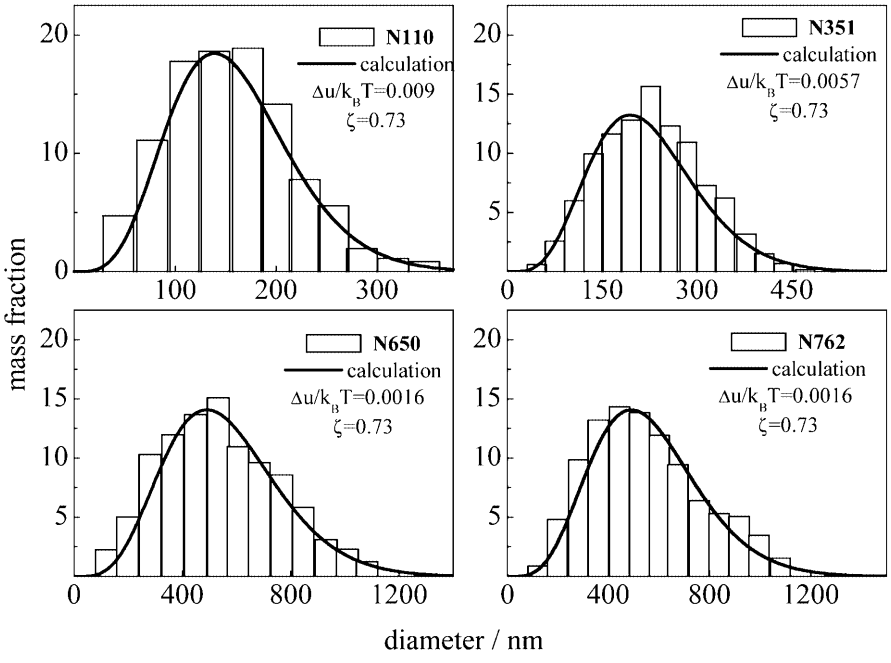

Fig. 2 Mass fraction of aggregates of oil furnace carbon blacks in the dry state as function of the diameter according to [3]. The *solid lines* are computed with the aid of Eqs. (10) and (14) with the parameters as indicated

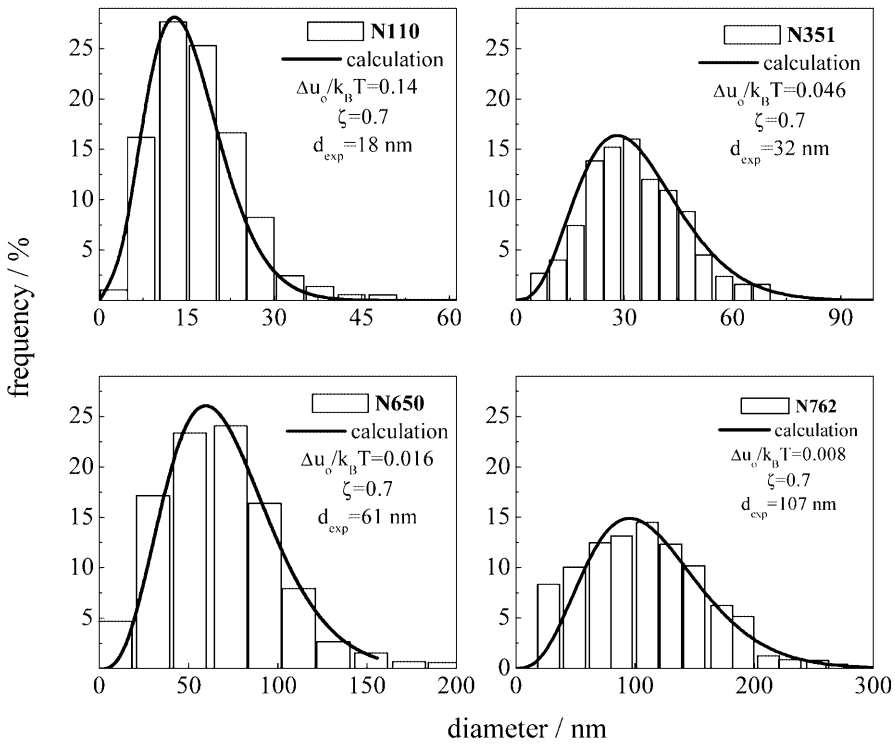

Fig. 3 Frequency of particles of oil furnace carbon blacks in the dry stage as function of the diameter according to [4]. The *solid lines* are computed with the aid of Eqs. (9) and (14) with the parameters as indicated

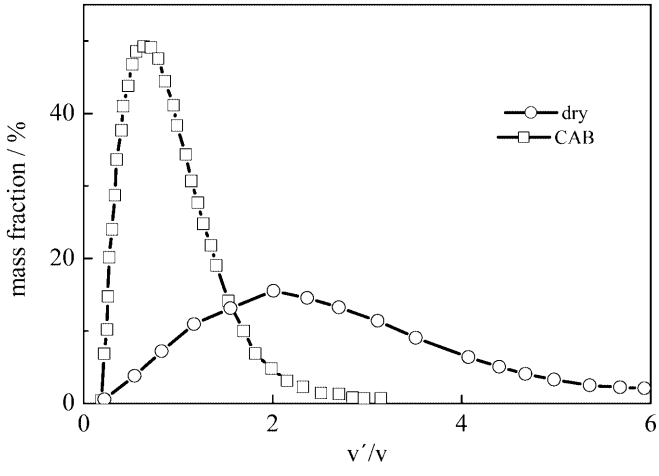

Fig. 4 Distribution of ν'/ν for N358 in CAB chip relative to the dry state according to [8]

Internal equilibrium within the aggregates should rapidly be established.

Reversible aggregation can then be described by considering a set of quasi-chemical reactions defined by the kinetic equations [9]

$$\begin{aligned} &m_1 + m_1 \leftrightarrow m_2 : [m_2] = K[m_1]^2 \\ &m_2 + m_1 \leftrightarrow m_3 : [m_3] = K[m_2][m_1]^2 = K^2[m_1]^3 \\ &\cdots\cdots\cdots\cdots\cdots\cdots\cdots\cdots \\ &m_{y_a-1} + m_1 \leftrightarrow m_{y_a} : \left[m_{y_a}\right] = K\left[m_{y_a-1}\right][m_1] = K^{y_a-1}[m_1]^{y_a} \end{aligned} \tag{1}$$

where m_1 is the mass of the primary particles and $[m_1]$ is the molar concentration of particles in the liquid state with a defined fraction of excess free volume ($[m_1] < 1$). m_{ya} gives the mass of aggregates comprised of y_a units; the concentration of these aggregates is $[m_{ya}]$. For each of the many reactions the constant K is the same. K should not depend on the composition, of course, on temperature or pressure.

Accounting for the conservation of mass

$$N_o[m_1]\sum_{y_a=1}^{\infty}(K[m_1])^{y_a-1} = 1 \tag{2}$$

where N_o is the normalization constant; we are led to the molar fraction $n(y_a)$ ("Schulz-Flory" distribution) [10, 11]

$$n(y_a) = (1-x)x^{y_a-1} : x = K[m_1] \tag{3}$$

Dependent on the value of x this size distribution of aggregates may become very broad [9].

The thermodynamic formulation

To recall the thermodynamic formulation of the reaction constant K let us consider dimerization in a molecular gas. K is defined here by [12, 13]

$$\begin{aligned} &K = e^{-\beta\Delta f_o} = \frac{\xi_{M_2}}{\xi_{M_1}^2} : \beta = \frac{1}{k_B T} \\ &\xi_{M_1} = \sum_r e^{-\beta u_r(M_1)};\ \xi_{M_2} = \sum_r e^{-\beta u_r(M_2)} \end{aligned} \tag{4}$$

with Δf_o as standard free energy of a dimer. $u_r(M_i)$ is the energy of the excited state r of the molecule M_i. ξ_{M_i} is the quantum mechanical partition function of molecules M_i. Forming new molecules they store energy determined by the defined number of exited internal states.

If now aggregation should be treated in an analogous manner, aggregates must be considered as dynamic entities characterized by internal ''modes of motion''. Of course, the partition function of an aggregate as sum over the intra-aggregate modes of motion is not known at all. The processes include not only oscillations but also a continuous modification of the internal configuration. We proceed therefore by introducing the standard free energy of aggregation $\Delta f_o = \Delta u_o - T\Delta s_o$, i.e. the change of the free energy per unit when it is built in an aggregate with stationary internal properties. The probability function x in Eq. (3) then reads

$$x = K[m_1] = e^{-\beta(\Delta u_o - T\Delta s_o - k_B T\, ln[m_1])} \approx e^{-\beta\Delta u_o} \tag{5}$$

Since Δf_o does de facto not depend on temperature we have

$$\Delta s_o \approx -k_B 1n[m_1] > 0; [m_1] < 1 \tag{6}$$

The standard aggregation entropy Δs_o is positive since $[m_1] < 1$. There are good reasons for expecting that $\Delta s_o > \Delta u_o$ so that a negative standard free energy results. x equalizes to the Boltzmann factor. Combining Eqs. (3) and (5) the number of aggregates n_y is then deduced to be given by

$$\begin{aligned} n(y) &= C_o e^{-y\beta\Delta u_o} \\ C_o &= \frac{1}{\sum 1 - e^{-y\beta\Delta u_o}} = 1 - e^{-\beta\Delta u_o} \end{aligned} \tag{7}$$

where y gives the number of contacts within an aggregate comprised of y_a units ($y = y_a - 1$). According to the principles recalled in the Appendix [14] the entropy of this ensemble is maximum.

The standard energy

In all cases known to date the standard aggregation energy is positive. Let us explain this in terms of the increment model on hand of the sketch in Fig. 5. With the symbols indicated the standard energy may be written as

$$\begin{aligned} y\Delta u_o &= y(u_{osc} + u_{con}) + 2u_e - (y+1)u_L \\ u_e &= \chi u_L \\ y\Delta u_o &= y(u_{osc} + u_{con}) + (2\chi - y - 1)u_L \\ \Delta u_o &\approx (u_{osc} + u_{con}) - u_L \end{aligned} \tag{8}$$

The negative contact energy between two units (u_{con}), the ''excess energy of the ends'' (u_e) as well as the positive value in the state of reference u_L should fall in the region of $k_B T$ as a necessary condition for ''reversible aggregation''. Within the aggregates many modes of motion should be excited this way storing kinetic and potential energy (u_{osc}). For positive values of Δu_o the energy of the ''internal modes'' (u_{osc}) must exceed the sum of the negative contributions. Hence, aggregates are dynamic metastable entities with fluctuating dissipative internal properties; they store energy.

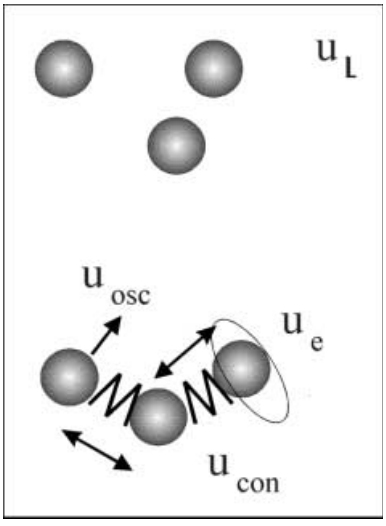

Fig. 5 Sketch of the formation of an aggregate comprised of three units in terms of an increment model. u_{con} is the contact energy per unit, u_e the one of an end group. u_{osc} gives the mean internal energy per unit stored by internal modes of motion. u_L should define the internal energy of a unit in the state of reference without any contacts

A relevant extension

The entropy of an aggregate ensemble depends on the ''internal freedoms'' of the fluctuation dynamics. This should be accounted for by extending Eq. (7) [8]:

$$n(y) = C_n y^p e^{-y\beta\Delta u_o} \tag{9}$$

where C_n is the normalization constant. It is shown below that the parameter p seems to characterize the ensemble entropy.

The mass fraction of aggregates (de facto identical with the volume fraction) h_u (y) is obtained by multiplying the relation in Eq. (9) with y:

$$h_u(y) = C_h y^{p+1} e^{-y\beta\Delta u_o} \tag{10}$$

where C_h is the normalization constant. The width of these distributions grows if the temperature is raised or if the standard aggregation energy is diminished (Fig. 6).

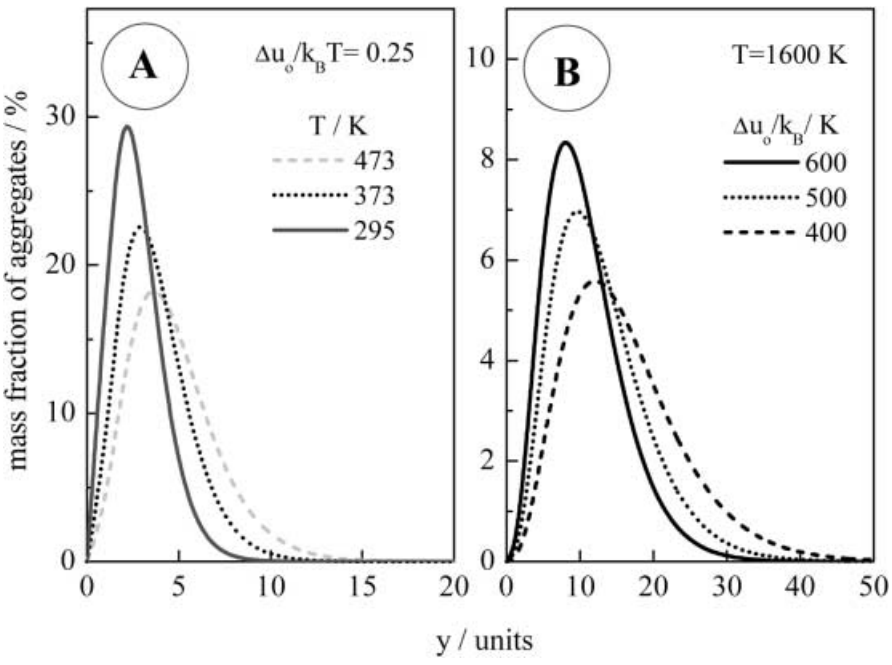

Fig. 6A,B Mass fraction of aggregates as function of units y: **A** at different temperatures; **B** for different standard aggregation energies computed with Eq. (10)

The mean size of the aggregates $\langle y \rangle_p$

$$\langle y \rangle_p = \frac{\int_{y=0}^{\infty} y^{p+1} e^{-y\beta\Delta u_o} dy}{\int_{y=0}^{\infty} y^{p} e^{-y\beta\Delta u_o} dy} = \frac{p+1}{\beta\Delta u_o} \tag{11}$$

is predicted to grow with T (Fig. 6A) depending inversely on the standard aggregation energy (Fig. 6B).

Universality

Introducing the variable $\eta_y = \beta y \Delta u_o$ into Eqs. (9) and (10) we are led to the universal relations

$$\begin{aligned} n_u(y) &= \frac{n(\eta_y)}{C_n} (\beta\Delta u_o)^p = \eta_y^p e^{-\eta_y} \\ h_u(y) &= \frac{h(\eta_y)}{C_h} (\beta\Delta u_o)^{p+1} = \eta_y^{p+1} e^{-\eta_y} \\ \eta_y &= y\beta\Delta u_o \end{aligned} \tag{12}$$

Ensembles installed by reversible aggregation are thus characterized by the following the criteria:

1. Different "classes" of aggregate ensembles should be typified by the value of the parameter p
2. The reduced aggregate size distributions of the same class should fall on a "mastercurve" (Eq. 12) (universality)
3. The mean size of the aggregates, i.e. the width of the size distributions, should be controlled by the factor $1/\beta\Delta u_o$ (Eq. 11)

Hence, the reliability of the model is straightforwardly tested by describing appropriate experiments.

The parameter *p*

It is a significant matter that the value of the parameter p seems to depend on the ensemble entropy the value of which should typify the fluctuation-dissipation behaviour of the whole aggregate ensemble.

For ensembles comprised of aggregates with an anisotropy which does not depend on the size p should be equal to zero. The number distribution is then given by Boltzmann's distribution. Continuous production and decomposition of the whole configuration installs a defined metastable stationary aggregate size distribution which is usually very broad since the ensemble entropy should be maximized.

Yet the internal anisotropy of aggregates may increase with y. This is expected for aggregates with an anisotropic shape where the number of internal modes of motion grows with the size of the aggregates. To calculate the density of orientation states we plot as shown in Fig. 7 $\Delta u_{cy}/\Delta u_{co} = y$ against the vector $\boldsymbol{k}(y)/k_o = y\boldsymbol{e}$ The length of $\boldsymbol{k}(y) = yk_o\boldsymbol{e}$ (e unit vector in direction of principle axis) describes that the anisotropy grows proportional to y. The orientation entropy is maximum if the anisotropic cells are randomly oriented. Yet the anisotropy of the cells is not a polar property. For a "two-dimensional ensemble" the density of aggregates with y contacts should thus be proportional to half of the periphery of the circle with the radius of y (Fig. 7). In this case p should be equal to 1.

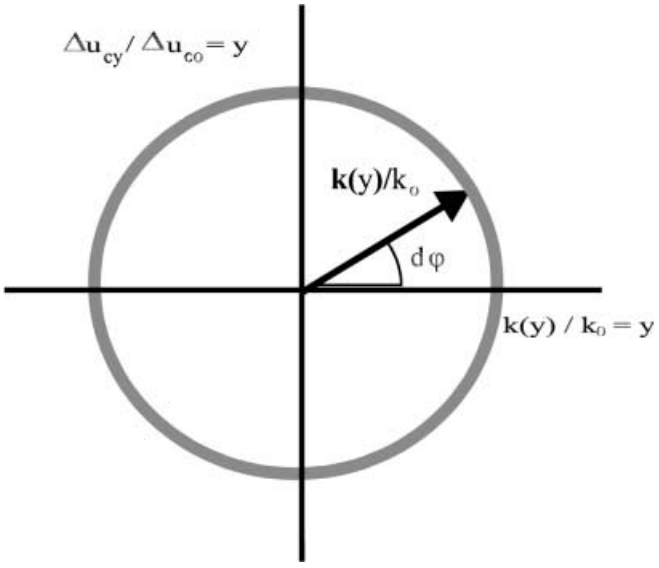

Fig. 7 The *grey circle* gives the density of orientation of a two-dimensional system of randomly oriented aggregates the anisotropy of which increases with y

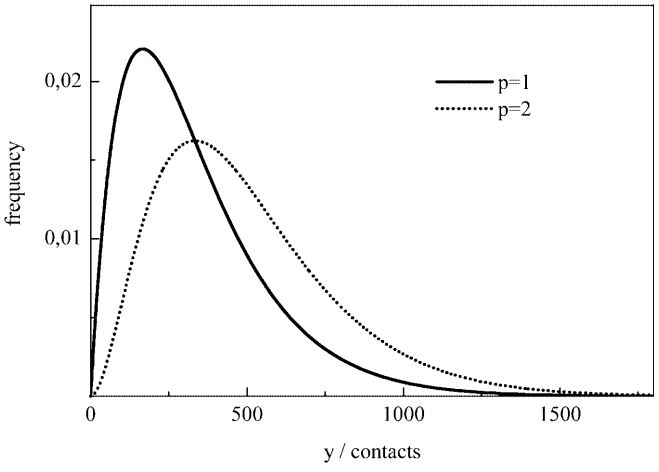

Fig. 8 Frequency as function of the number of contacts per aggregate for $p=1$ and $p=2$

In bulk the density of aggregates with y contacts should be proportional to y^2 (given by half of the surface of a sphere with the radius y in the $(k(y)/k_o - u_{cy}/u_{co})$-space). The parameter p should be equal to 2.

Hence, the front factor in Eq. (9) seems to typify extra "freedoms" of the ensemble entropy which increase the density of states. The two representative examples drawn out in Fig. 8 demonstrate that the width of the size distribution increases with p, i.e. with the ensemble entropy.

A generalization

The actual size distribution of an aggregate ensemble is determined by the value $\beta\Delta u_o$ is assigned to (Eq. 9). In the above model $1/\beta = k_B T$ gives the mean energy stored via continuously running thermally activated processes. Fluctuations come about if $\beta\Delta u_o < 1$. Observed values are much smaller covering a range of about $0.01 > \beta\Delta u_o > 0.002$ [15].

Yet our mode1 demands only that the configuration of the aggregate structure should fluctuate. Stationary ensemble structures may thus even so be generated if the underlying processes are excited otherwise. Representative examples are simple living systems like bacteria or yeast [15]. Fluctuations of the cell size distributions or the inter-cell structure are here mainly activated via "enzymatically driven chemical reactions". The production and decomposition of proteins occurs including covalent peptide bonds with a relatively large energy [16]. Interpreted in terms of the increment model of aggregation the standard energy Δu_o is thus much larger than $k_B T$. It is now significant that the cell size distribution is described by assigning $\beta\Delta u_o$ to values in the same range as above [15]. Hence, intermediate states excited during the continuously running enzymatically activated complex reactions should store, on average, amounts of energy which exceed the large value of Δu_o. Moreover, dissipation-fluctuation processes seem to show the same features as thermally activated processes since the typical symmetries of the model of reversible aggregation also characterize the cell ensembles of bacteria or yeast. This encouraged us to describe the properties of particle and aggregate ensembles of carbon blacks analogously.

Computer simulations

Computer simulations are an excellent tool for studying aggregation phenomena also by using well known differential equations which have not yet been solved. Quasi-stationary behaviour should be recognized.

A model of cluster aggregation is introduced by Kolb [17] where clusters can both aggregate and fragment. This model is the reversible counterpart to diffusive clustering of clusters. Stationary equilibrium requires that the aggregation time is equal to the fragmentation time. It is evidenced with the plot in Fig. 9a that the reduced simulated distribution is fairly well reproduced by using Eq. (12) with $p=1$. This supports the suggestion of Kolb [17] that while a particular aggregate may have a relative weight that depends on the kinetics, the scaling properties are universal.

Investigations of the connection between the geometry of clusters and the kinetics [18] deliver the reduced size distribution of aggregates $(n(y) = y^2 n_y;\ y_r = y/\langle y \rangle)$ by

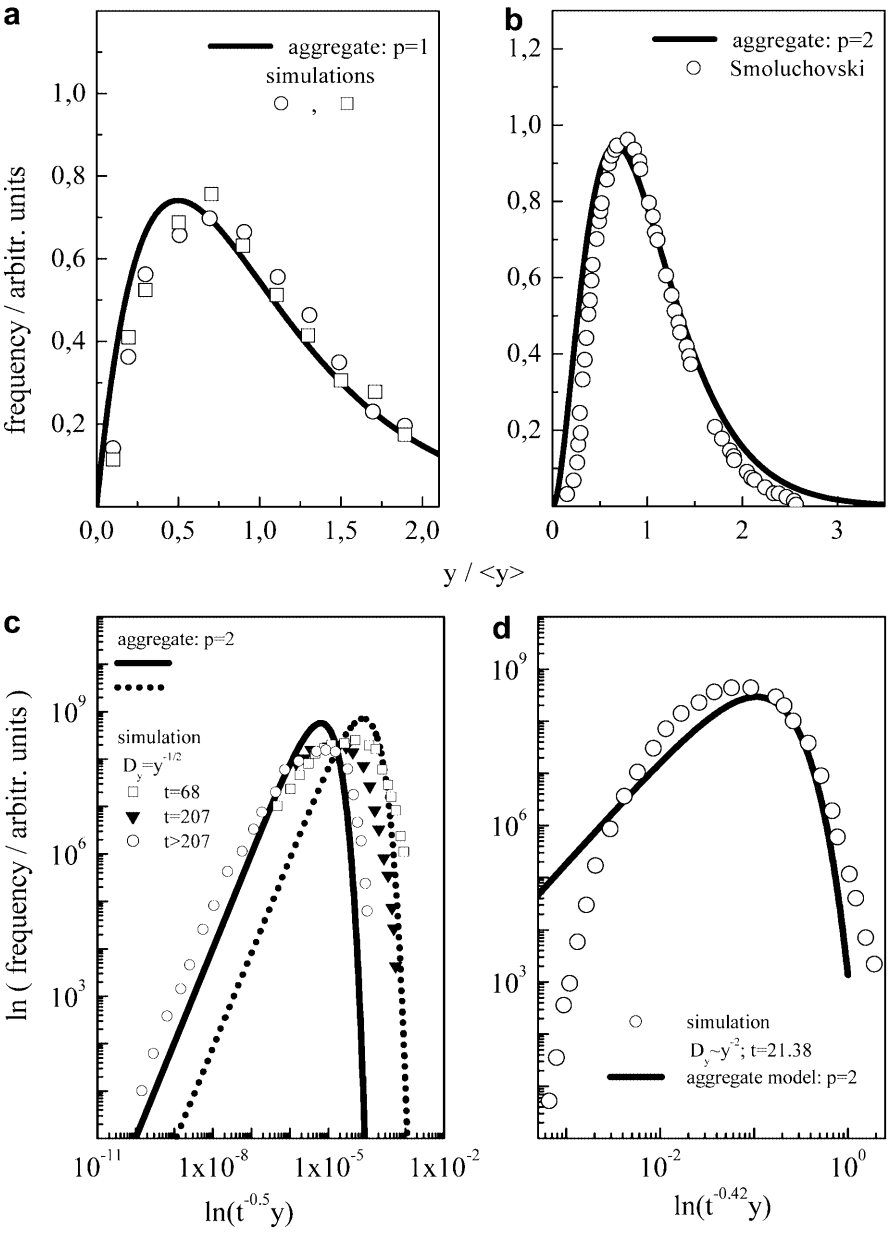

Fig. 9 **a** Reduced two-dimensional size distribution of the aggregates as function of $y/\langle y\rangle_{d=2}$ installed by of reversible cluster-cluster aggregation in the stationary limit obtained by a computer simulation model of by Kolb [17]. The *solid line* is computed with the use of the Eq. (11) and $p=1$. **b** Reduced number distribution of aggregates of different size as function of $y/\langle y\rangle$ obtained by a numerical solution of the Smoluchovski equation [19] according to [20] (○). The *solid line* computed with Eq. (11) and $p=2$. **c** The time dependent aggregate-size distribution obtained from three-dimensional simulations with a diffusivity exponent $\gamma_c=-1/2$ and a particle concentration of $\varrho=0.0034$ according to [21]. The times t are indicated with the plot. The *lines* are computed with the universal relation defined in Eq. (11). The curve is shifted on the logarithmic scale accordingly. **d** The time dependent aggregate-size distribution obtained from three-dimensional simulations with a diffusivity exponent $\gamma_c=-2$ according to [21]. Representative times t are indicated with the plot. The *solid line* is computed with Eq. (12). The *curve* is shifted on the logarithmic time scale

using the Smoluchovski equation [19–21] (Fig. 9b). It is an important finding that the distribution calculated with Eq. (12) and $p=2$ reproduces the "Smoluchovski curve" (Fig. 9b). The deduced aggregate ensemble turns out to be identical with the universal stationary equilibrium pattern constituted by reversible aggregation while the size of aggregates grows in time. Apparently the system passes through a sequence of thermodynamically rapidly optimized "equivalent" ensembles [22]. This has the consequence that the entropy production is minimized.

The effect of cluster diffusivity on the cluster-size distribution studied via simulations by Meakin et al. [23, 24] can be recognized in Figs. 9c, d. The diffusion coefficient is defined by the power law

$$D \approx D_o y^{\gamma} \tag{13}$$

where D_o is a constant. The parameters used in the calculation are indicated with the plots $\gamma=-0.5$, $\gamma=-2$. For $\gamma=-1/2$ and at not too short times the cluster size distributions coincide with the stationary number distribution of the model of reversible aggregation computed with Eq. (12) ($p=2$). The diffusion coefficient depends here on the mass. Small clusters ("aggregates") move more quickly in randomly chosen directions than larger ones. Yet, agreement is not established for every set of the parameters (Fig. 9d).

All in all we are led to conclude that fluctuation-dissipation during the simulation seems to yield to cluster

ensembles where the configurational entropy is rapidly maximized. At not too short times quasi-stationary distributions are established showing the same shape as in the stationary limit of the model of reversible aggregation.

Comparison with experiments and discussion

Within the reactor at very high temperatures (1700–2100 K) dissipations-fluctuations behaviour of carbon blacks is now assumed to show analogous features as recognized in the above simulations. The dynamics and the rheological conditions should allow formation and annihilation of carbon black particles and aggregates.

At high temperatures structure and internal properties of particles or aggregates should differ from those at room temperature. Here, continuously running chemical reactions activated under extreme rheological conditions do not happen any more. Our analysis is therefore based on the hypothesis that each particle or aggregate ensemble registered at low temperatures should display the same "global structure" as in the reactor.

Particle size distribution

The formation of particles may occur via surface growth processes of nucleated soot particles by reversible cluster-clustering [25], [26]. This growth occurs via "microscopically reversible" attachment to, and incorporation in, existing species smaller than the first observable soot particles. Fragmentation of particles should also occur.

The identification of particles is confronted by problems [3] including the method by which the diameter of the particles d_{ya} in electron microscopic or AFM pictures is exactly related to the number of elements the particle is comprised of. We introduce the empirical relation

$$d_{ya} = 2y_{y_a}^{\zeta} l_o; y_a = y + 1 \tag{14}$$

where l_o scales the absolute value of the unit set here equal to 1 nm. For densely packed spherical particles in a cubic lattice the minimum value of the parameter ζ should be equal to 1/3. This value should increase for particles with a distorted more loosely packed internal structure.

The frequency distribution of carbon blacks with different mean diameters are depicted in Fig. 3 [4].The solid lines are computed with Eqs. (9) and (14) adjusting $\beta\Delta u_o$ and (the absolute heights are fitted straightforwardly). The mean diameters and the values of the parameters are indicated with the plot. $\beta\Delta u_o$ is, in any case, so small that reversible aggregation can be activated. Figure 10 shows that the mean size of the particles is inversely proportional to $\beta\Delta u_o$ (Eq. 11).

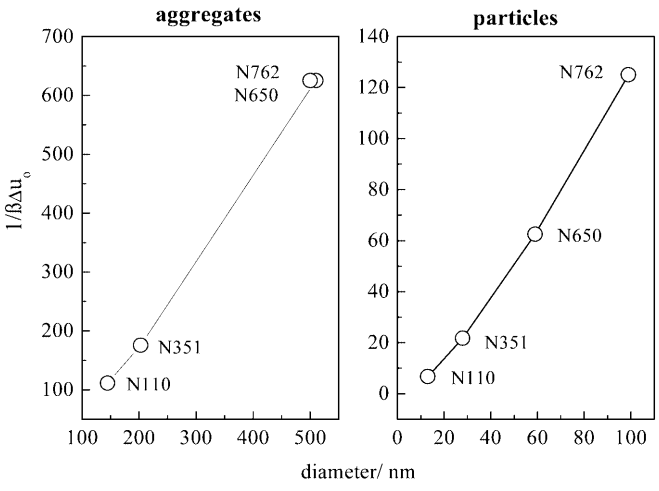

Fig. 10 $1/\beta\Delta u_o$ of particles and aggregates against the mean diameter for the carbon blacks as indicated

Plotted as function of the variable $\eta_y = \beta y \Delta u_o$ all the distributions fall on the universal curve which is not shown here. Hence, the criteria formulated above are altogether confirmed.

Different grades of carbon blacks seem to be typified by systematically changing values of $\beta\Delta u_o$. The standard aggregation energy shows the largest value for N110, i.e. for the type with the smallest mean particle size (diameter 18 nm) decreasing with the mean diameter of the particles (Fig. 10). Since X-ray studies [27–29] show for N110 the largest para-crystalline distortions of different carbon blacks one might suspect that the contact energy Δu_{con} between the units (which are not exactly identified) shows here its minimum value. If the dynamic energy u_{osc} remains about the same the standard aggregation energy of N110 $\Delta u_o = \Delta u_{osc} - \Delta u_{con}$ should be maximum.

The range covered by ζ (0.7–0.72) is about the same for the different types of carbon blacks indicating that the density of particles should not correspond to a compact pattern.

Aggregate size distribution

In Fig. 2 the mass fractions of aggregates of the same different dry carbon blacks as above [3] are plotted against the diameter. The data are fairly well fitted with the aid of Eqs. (10) and (14). The parameters are indicated with the plots. The relative standard aggregation energies are sma1ler than those deduced for particles, also decreasing systematically with the mean size of the aggregates (analogously to the behaviour of particles) (Fig. 10). The width of the stationary size distribution of aggregates decreases the smaller the particles are (Fig. 11). In the reduced version they fall on

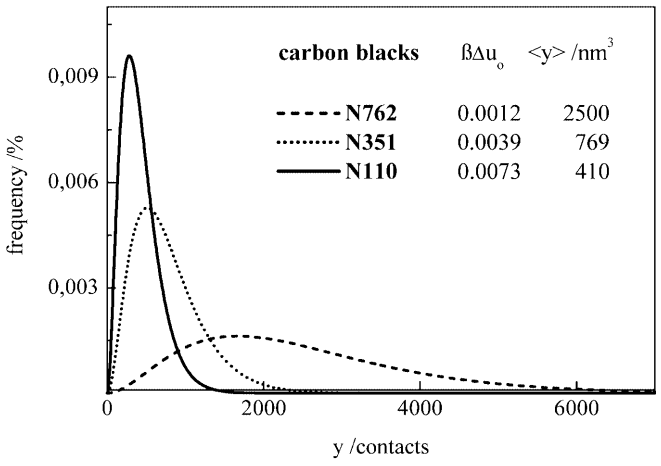

Fig. 11 The frequency distributions as function of the size of the aggregates (y) for different carbon blacks as indicated

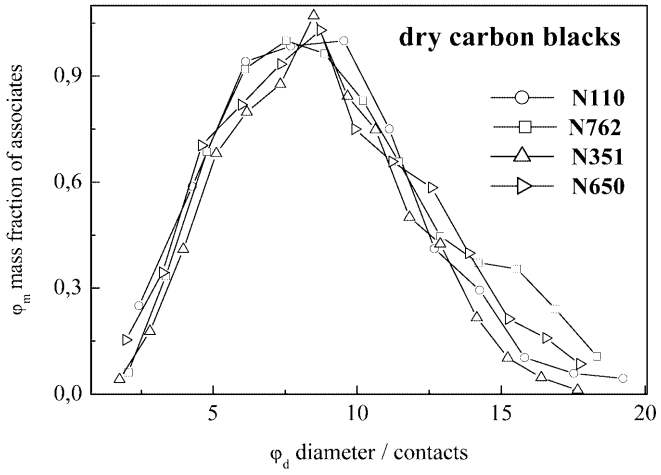

Fig. 12 Master curve of the data of dry carbon blacks as indicated; φ_d and φ_m are assigned to values so that height and position of the maximum of the different systems are fitted to the pattern of N110

a master curve. This is demonstrated with the plot in Fig. 12 where position and height of the maxima of the different patterns are adjusted to each other. The criterions formulated above are fully confirmed.

All in all, these results support the idea that particle and aggregate ensembles should de facto optimize themselves independently. The "momentary" mass fractions of both particles and aggregates are likely to differ from their optimum values. An analogous behaviour has been observed in a completely different system. Defects at the surface of metal crystals under stress [30] constitute, for example, a fluctuating hierarchical defect structure produced by reversible aggregation of dislocations which move within conservative sliding planes of the crystals. The reduced size distributions of the defect generations are at each moment identical with their stationary patterns. However, the concentrations of both ensembles seem not to have arrived at final stationary values.

CAB-treated samples

We discuss now the aggregate size distribution of CAB-chip dispersions [4], [8] (Fig. 4). Let us assume that the original aggregates are fragmented. The particles themselves should operate as rigid entities. New aggregates are thus only generated and decomposed [2], [3].

We apply our generalized version of the model of reversible aggregation where $1/\beta$ should characterize the mean energy stored via dissipative fluctuations during the CAB-procedure which includes a milling process. During the CAB-process a stationary aggregate ensemble should rapidly be build up. The special processing conditions including "viscoelastic" activation may be characterized by defining an "effective temperature" $T^* > T$. The new stationary aggregate ensemble is formally considered as a pattern which would be generated via thermal activation at the elevated temperature T^*.

The above suggestion is now tested by describing the aggregate ensembles the structure of which is determined by a method which goes back to Medalia [31]. For each aggregate he defined an equivalent sphere $v_{\mathrm{eq}}(y)$ based on the measured projected area in the TME-image, each one represented by a circle. With the approximation $y_{\mathrm{a}} \approx y$ the ratio $v'(y)/v$ is then equal to

$$\frac{v'(y)}{v} = \frac{v_{eq}}{y} \tag{15}$$

Many aggregates reveal now that they seem topologically to behave analogously to a "coiled chain" (Fig. 1). Different "chain-like" conformations can also be recognized in the TME-images [32] shown in Fig. 13. It is thus suggested to define the equivalent volume of an aggregate with y by introducing the well known power law which relates to the chain-end-to-end distance [33, 34]

$$v_{eq} \propto y^{3\kappa} \tag{16}$$

The maximum entropy (as for a phantom chain with y units) should be arrived at if κ is equal to 1/2 [33–35]. Yet at stationary equilibrium the mean shape of aggregates should result from a balance of entropy effects leading to a kind of branched random walk structure where excluded volume forces favour aggregate expansion. κ is thus likely to attain values much larger then the minimum value of the phantom chain (1/2).

Combining Eqs. (15) and (16) we are led to

$$\frac{v'(v)}{v} = \frac{v_{eq}}{y} = y^{3\kappa-1} \tag{17}$$

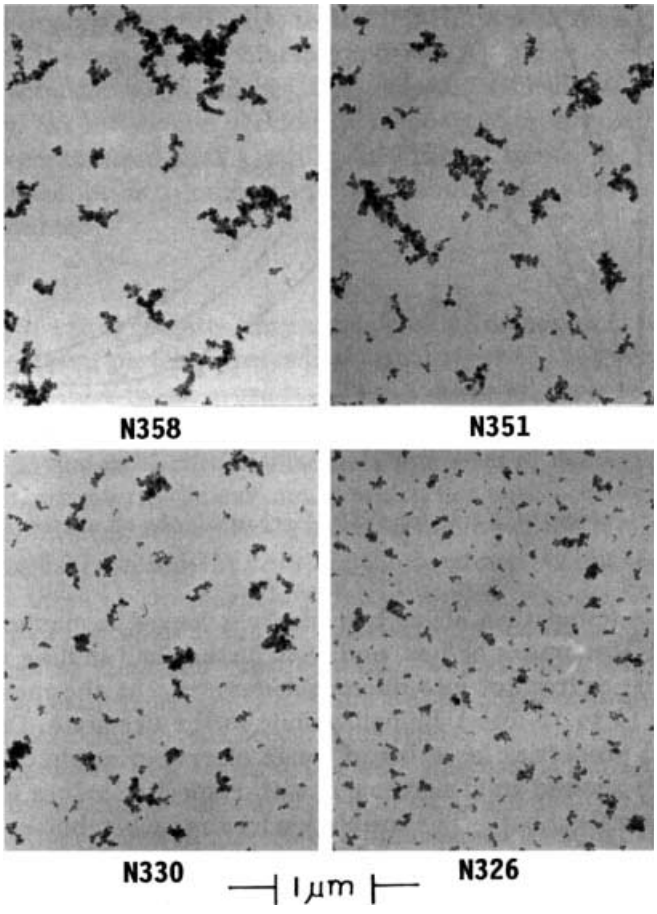

Fig. 13 TEM images of the carbon blacks as indicated according to [32]

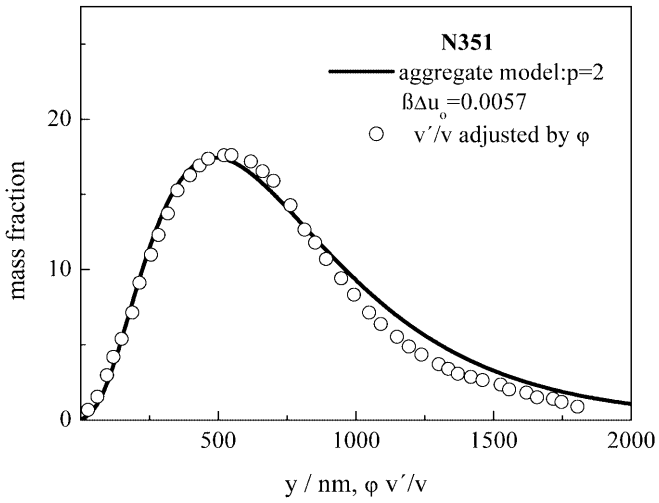

Fig. 15 v'/v scaled by φ so as to compare with the mass distribution computed with Eq. (18) and the parameters as indicated. These parameters agree with the ones given in Fig. 3

The mass fraction of aggregates with y contacts is then according to Eq. (6) equal to

$$h(y) = C_v y^3 e^{-\beta y \Delta u_o} \tag{18}$$

with C_v as normalization constant.

The mass fractions of aggregates for different types of carbon blacks of varied amounts of oil (di(*n*-dibutyl) phthalate, DPB) as function of v'/v are depicted in Fig. 14 [32]. The solid lines are computed with Eqs. (17) and (18) and the parameters $\beta\Delta u_o$ and κ as indicated with the plot. The relative standard aggregation energy

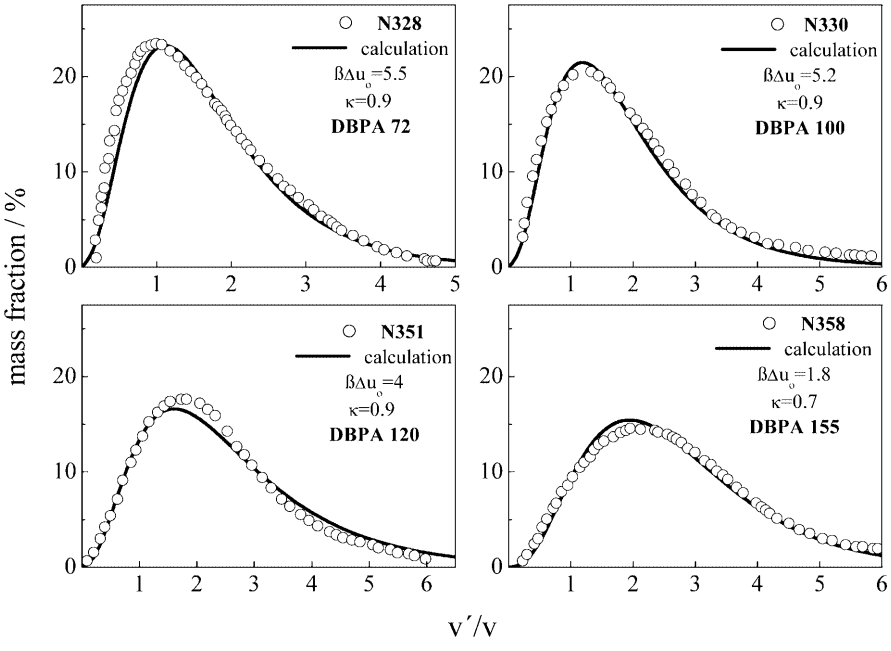

Fig. 14 Mass fraction aggregates of the different carbon blacks computed with Eqs. (17) and (18) and $\beta\Delta u_o$ and κ as indicated

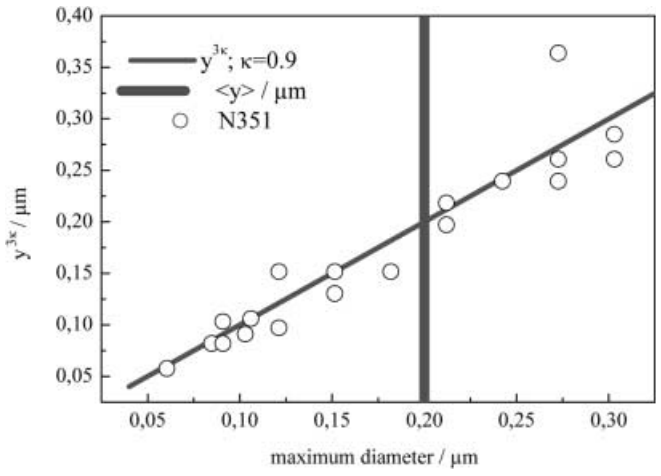

Fig. 16 y plotted against the experimental maximum diameter of the aggregates deduced from an analysis of the TME-image of N351 depicted in Fig. 13

$\beta\Delta u_o$ tends to decrease with increasing amounts of DBPA showing altogether relatively large values as the consequence that $v'(y)/v$ is not related to the size of the units. Yet the plot in Fig. 15 reveals that the equivalent volume scaled by the factor turns out to be proportional to the volume occupied by the aggregates themselves (y). The solid line is here computed with the value of $\beta\Delta u_o$ as obtained by the fit of the data in Fig. 2.

For the different carbon blacks involved here κ is equal to 0.9 with the exception of N335 where κ drops down to the smaller value of 0.7. According to the images depicted in Fig. 13 this agrees with the qualitative recognition that the aggregates of N358 appear not to be extended so much as is observed for all the other patterns. All in all, aggregates should exhibit a defined anisotropic stationary shape constituted by branched configurations (Fig. 1) [3]. Related to the entropy maximum configuration the anisometry may be characterized by

$$r = e^{3(\kappa-0.5)} \tag{19}$$

For the systems involved r covers here the range $1.7 < r < 1.8$. These values are near to the one of aggregates in liquids where r is about $1.5 < r < 1.6$. The conformational entropy of the aggregates is really maximized in analogy to the behaviour of polymer chains [33, 34, 36]. It is indicated with the plot in Fig. 16 that the maximum extension of the aggregates of N351 shown in Fig. 13 corresponds indeed to only slightly "coiled patterns" described by Eq. (16) with $\kappa = 0.9$, i.e. the exclusion volume of the particles extends each aggregate substantially. This plot documents also that the conformations of the aggregates of different size seem separately to be adjusted so as to maximize the conformational entropy.

After the CAB-treatment the size of the aggregates is substantially reduced [3]. This is demonstrated in Fig. 17A where the mass distribution of a dry ensemble is compared with that of a CAB-treated system. The data can be fitted with Eq. (18) if $T^* = 1600\ K$ is replaced by $T^* = 680\ K$. $\beta\Delta u_o$ is increased by a factor of $1600/680 = 2.35$ so that the mean aggregate size of the CAB-ensemble is reduced accordingly (Eq. 11).

Plotted in a reduced version (Fig. 17B) the shapes of the original pattern and the CAB-treated sample are verified to be identical, i.e. rheologically activated quasi-reversible aggregation should really be enforced during the CAB-procedure.

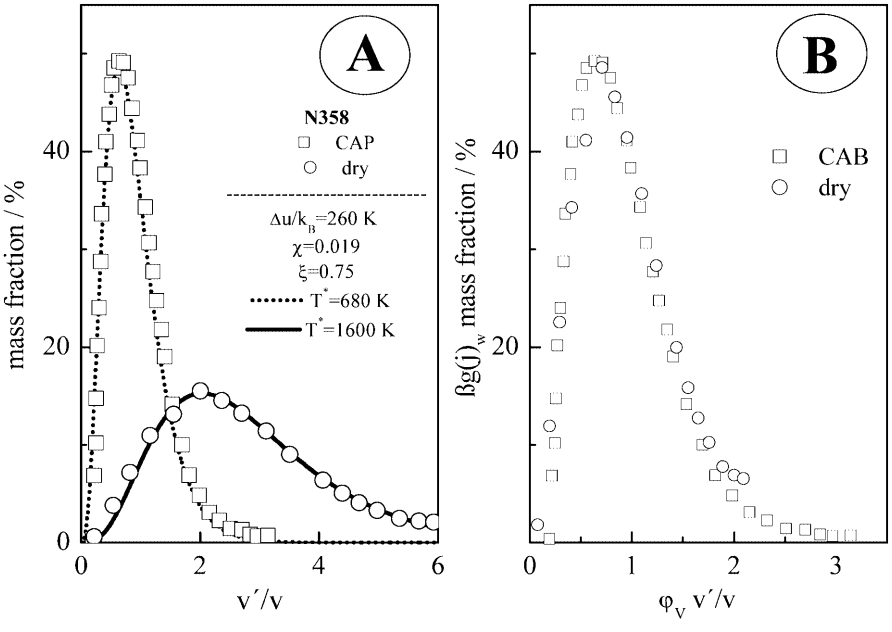

Fig. 17 **A** Mass distribution of v/v for N358 in CAB chip relative to the dry state according to [8]. *Solid and dashed lines* are computed with Eqs. (17) and (18). The parameters are indicated (N358: dry $T^* = 1600$ K and CAB chip $T^* = 680$ K). **B** Both distribution adjusted to the same maximum position (φ_v) and to the same height

Conclusions

The formation of aggregate ensembles with a statistically defined colloid-structure needs fluctuation-dissipation processes. Due to the finite lifetime of each configuration a sequence of generations is developed in the course of time. Each of them is characterized by a statistically identical stationary ensemble structure with universal features. These properties can be described with the model of reversible aggregation (as a typical increment conception). The model is based on the equivalent importance of energy and entropy. At constant energy (disposed by the number of possible contacts between the units) the ensemble entropy is maximized via quasi-continuously occurring production or decomposition of iso-energetic ensemble configurations.

Relevant is the conception to consider aggregates as ''inhomogeneous micro-phases'' [37] which store dynamic energy via internal modes of motion like oscillations or configurational fluctuations. This leads to positive values of the standard aggregation energy. The intra-aggregate fluctuations are one of the factors which limit the life time of each aggregate. It is shown elsewhere [38] that these fluctuations guarantee that internal equilibrium is established by adjusting the intra-aggregate entropy accordingly (condition of ''saturation''). Aggregates should thus be considered as metastable micro-phases with universal liquid-like internal properties.

The whole ensemble entropy thus turns out to be an important factor in organizing ''dissipative systems'' with optimized metastable colloid-structures with unique universal properties in each class. Controlled by the extremum principles of thermodynamics they keep their ''statistical identity'' in the course of time since they pass through a sequence of statistically identical realizations. Even for different systems the reduced representations are identical within each class ($p = 2$: carbon blacks and aggregates in liquids; $p = 3$: bacteria and yeast cell ensembles; $p = 1$: length distribution of the proteins within the cells of bacteria and yeast).

It is a crucial finding that the size distributions of aggregate ensembles derived via computer simulations determined at not too short times turn out to be identical with the universal pattern of the belonging model of reversible aggregation (Fig. 9). Each of these patterns seems to constitute in comparably short times quasi-stationary ensemble structures. They seem to be a hallmark even of stationary irreversible processes [22] running off in systems with a fluctuating colloid structure.

This phenomenon explains why the hierarchically organized particle and aggregate ensembles of carbon black ensembles can be represented with our model. The ensembles exhibit unique properties both belonging to the class $p = 2$. Each of them seems nearly independently

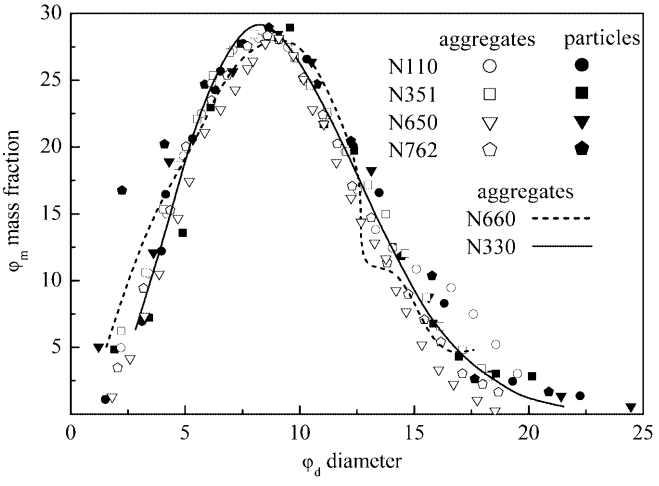

Fig. 18 The intensity adjusted master-curve of the mass fraction of particles and aggregates of the various carbon blacks as indicated with the plot as function of the reduced aggregate diameter

to be built up via analogous fluctuation-dissipation processes. This hypothesis is also supported with the reproduction of the aggregate size distribution of the ''CAB-pattern'' where the particles operate as solid entities. At constant energy the entropy of ensembles is, in any case, maximized, indicated by the typical asymmetric shape of the distributions. Universality is finally, once more, demonstrated with the plot in Fig. 18 where it is to be seen that the reduced distributions of both particles and aggregates are really identical for all the different grades of carbon blacks studied here. A solid explanation of the conditions is wanted which must be fulfilled so that hierarchic ensemble structures of the type involved here are organized.

A remarkable result of this paper is, in our opinion, that metastable ensemble structures can be installed in different ways, for example, activated in presence of continuously and collectively running quasi-reversible chemical reactions. These ensemble structures exhibit even during stationary irreversible processes for each class the same universal properties as observed for analogous aggregate ensembles where the dissipative structural fluctuations are thermally initiated. The topological structural features of all of them are identical, independent of how production and decomposition of the relevant entities are realized (thermal activation, enzymatically driven reactions, chemical reactions, viscoelastic processes). ''Reversible aggregation'' generates in any case stationary colloid structures which are unique and perfect. After any distortion a representative stationary pattern is rapidly recovered, i.e. these systems are ''self-healing''.

Cell ensembles of bacteria or yeast seem to behave analogously [39]. The distribution of the size of the cells

as well of the length of the intra-cell proteins can be shown to be "maximum entropy patterns" with universal properties.

Appendix. The Entropy Maximum Principle

Montroll and Shlesinger [14] used Boltzmann's entropy function H

$$H = -\int n(y)\ln(n(y))dy$$
$$\int n(y)dy = 1 \tag{A1}$$

By the method of Lagrange multipliers one seeks the distribution n(y) that maximizes the entropy subject to the auxiliary conditions

$$\int F_i(y)n(y)dy = c_i; F_1(y) = 1 \tag{A2}$$

We arrive at

$$\delta F(y) = -\int [\ln(n(y)) + \lambda_1 + \lambda_2 F_2 + \lambda_3 F_3]\delta n(y)dy = 0$$
$$\lambda_1 = -\ln C; \lambda_2 = 1, F_2 = \beta y \Delta u_o; \lambda_3 = -1, F_3 = \ln y^2 \tag{A3}$$

Constancy of the energy leads to the Boltzmann distribution. The front factor y^2 in Eq. (9) results for an ensemble comprised of aggregates the anisotropy of which grows with their size. Differently oriented aggregates of the same size y are "distinguishable". The orientation entropy of the aggregate ensemble is maximized if the aggregates are randomly oriented.

References

1. Donnet JB, Bansal RC, Wang MJ (1993) Carbon black. Marcel Dekker, New York Basel Hong Kong
2. Donnet JB, Voet A (1976) Carbon black. Marcel Dekker, New York Basel
3. Hess WM, Herd CR (1993) In: Bonnet BJ, Bansal RC, Wang MJ (eds) Carbon black. Marcel Dekker, New York Basel Hong Kong, p 89
4. Hess WM, McDonald GC (1979) Rubber Chem Technol 56:892
5. Bansal RC, Donnet JB (1993) In: Bonnet BJ, Bansal RC, Wang MJ (eds) Carbon black. Marcel Dekker, chap 2
6. Lahaye J, Ehrenburger-Dolle F (1993) The 2nd International Conference on Carbon Black. Mulhouse
7. Wagner HG (1981) In: Siegela DC, Smitter GW (eds) Particulate formation during combustion. Plenum, New York. p 1
8. Herd CR, McDonald GC, Hess WM (1991) Rubber Chem Techno165:1
9. Kilian HG, Metzler R, Zink BJ (1997) J Chem Phys 107:8697
10. Schulz RC (1939) Z Phys Chem B43:25
11. Elias HG (1971) Makromoleküle. Hüthig and Wepf-Verlag, Basel-Heideberg
12. Reif F (1965) Statistical and thermal physics. International Student Edn. McGraw-Hill-Cogakusha Ltd, Tokyo
13. Moore WJ, Hummel DO (1973) Physikalische Chemie. deGruyter, Berlin New York
14. Montroll EW, Shlesinger MF (1983) J Stat Phys 32:209
15. Kilian HG, Koepf M, Vettegren VI (2001) Prog Colloid Polym Sci 117:181
16. Alberts B, Bray D, Johnson A, Lewis J, Raff M, Roberts K, Walter P (1997) Essential cell biology. Garland, New York London
17. Kolb M (1986) J Phys A 19:263
18. Jullien R (1990) New J Chem 14:239
19. Van Smoluchovski M (1916) Phys Z 17:585
20. Botet R, Jullien R, Kolb M (1984) Phys Rev A 30:2150
21. Meakin P, Vicsek T, Family F (1985) Phys Rev B 31:564
22. Haase R (1963) Thermodynamik der irreversiblen Prozesse. Fortschritte der Physikalischen Chemie, Vol. 8. Steinkopff, Darmstadt
23. Meakin P (1985) Phys Rev B 31:564
24. Lin MY, Lindsay HM, Weitz DA, Ball RC, Klein R, Meakin P (1989) Nature 339:360
25. Tanner SD, Goodings SM, Bohme DK (1981) Can J Chem 59:760
26. Harris SJ, Weiner AM (1984) Combust Sci Technol 38:75
27. Heidenreich RD, Hess WM, Bann LL (1968) J Appl Cryst 1:1
28. Peng W, Strauß M, Pieper T, Kilian HG (1993) Mol Phys 80:419
29. Donnet JB, Custodero E (1993) In: Bonnet BJ, Bansal RC, Wang MJ (eds) Carbon black. Marcel Dekker, chap 5
30. Kilian HG, Vettegren VI, Svetlov VN (2000) Phys Solid State 42:2024
31. Medalia AI (1970) J Colloid Interface Sci 32:115
32. Herd CR, McDonald GC, Hess M (1991) Rubber Technol 65:1
33. Flory PJ (1953) Principles of polymer chemistry. Cornell Univ Press, Ithaca New York
34. Treloar LRG (1958) The physics of rubber elasticity, 2nd edn. Clarendon Press, Oxford
35. Mark JE, Erman B (1988) Rubberlike elasticity: a molecular primer. Wiley, New York Chichester Brisbane Toronto Singapore
36. Holzmüller W (1961) Physik der Kunststoffe. Akademie Verlag, Berlin
37. Kilian HG (1986) Prog Colloid Polym Sci 72:60
38. Koepf M, Kilian HG (1999) Acta Polym 50:109
39. Van Smoluchovski M (1916) Phys Z 17:585